Reaction Chemistry & Engineering

ROYAL SOCIETY OF CHEMISTRY

PAPER

View Article Online
View Journal

Cite this: DOI: 10.1039/d5re00535c

Anion size-dependent carbon dioxide adsorption capacity in high-purity diallyldimethylammonium-based poly(ionic liquid)s

Kohei Okubo, [a] Showa Kitajima,[ab] Hitoshi Kasai, [a] Kiyotaka Maruoka,[c] Yuta Takahashi,[c] Yoko Teruuchi,[c] Minoru Takeuchi,[c] Kazuhiko Igarashi[c] and Kouki Oka *[ade]

Received 4th December 2025,
Accepted 8th March 2026

DOI: 10.1039/d5re00535c

rsc.li/reaction-engineering

Poly(ionic liquid)s (**PIL**s) are solid materials composed of cationic or anionic polymers combined with counter ions. **PIL**s are investigated and applied as CO_2 adsorbents because they possess both the high CO_2 affinity of ionic liquids and the excellent stability and processability of polymeric materials. This work explored the correlation between the type of anion in **PIL**s and their CO_2 adsorption capacity *via* anion-exchange. As the skeleton of **PIL**s, we focused on poly (diallyldimethylammonium chloride) (**P[DADMA][Cl]**). Among the quaternary ammonium cations known to exhibit high CO_2 adsorption capacity, **P[DADMA][Cl]** contains the highest density of cationic sites, indicating the potential for further enhanced CO_2 adsorption capacity. However, conventional anion-exchange reactions often yield residual by-products in the resulting **PIL**s, making it difficult to reveal the inherent correlation between counter anions and CO_2 adsorption capacity. In this work, high-purity **PIL**s (**P[DADMA][AcO]**, **P[DADMA][TFMS]**, and **P[DADMA][SCN]**) without by-products were successfully prepared for the first time through careful dialysis. The CO_2 adsorption capacity of these **PIL**s increased in proportion to the size of the counter anion, and **P[DADMA][TFMS]** exhibited a seven-fold increase in the adsorption capacity compared to that of **P[DADMA][Cl]**. This work truly demonstrates that CO_2 adsorption capacity can be enhanced by designing the counter anions in **PIL**s.

Introduction

Ionic liquids are salts that exist as liquids at ambient temperatures, and are characterized by low volatility, high thermal and chemical stability, and the ability to design physical properties based on the combination of anion and cation species.[1–5] Meanwhile, poly(ionic liquid)s[6–9] (**PIL**s) are polymer materials composed of ionic liquids[10,11] as their building blocks. In particular, owing to their high solubility for carbon dioxide[12] (CO_2), they have good potential as CO_2 absorbents. While **PIL**s retain these excellent properties, they also possess mechanical stability and processability resulting from their polymerization.[13] Consequently, they have been extensively investigated for practical applications such as gas separation membranes[14] and solid adsorbents.[15]

Among **PIL**s, those with a quaternary ammonium cation skeleton are known to exhibit higher CO_2 adsorption capacities than **PIL**s with other imidazolium or pyridinium cation skeletons.[16] The CO_2 adsorption capacities of **PIL**s are expected to depend significantly on their anion species as well as the cation skeletons.[17] Therefore, the CO_2 adsorption capacity of **PIL**s containing various anion species introduced *via* anion-exchange reactions,[18] where the halides of **PIL**s react with the inorganic salts of each anion, has been revealed.[19,20] However, conventional anion-exchange reactions involve difficulty in completely separating the resulting **PIL**s from the by-product inorganic salts, and residual metal ions derived from the inorganic salts have been overlooked.[21] The residual metal ions in the **PIL**s prevent the evaluation of the influence of the counter anion on the CO_2 adsorption capacity.[22]

In this work, we aim to resolve these issues by performing precise purification by dialysis[23] and clarify the correlation between the type of anion in **PIL**s and their inherent CO_2 adsorption capacity. In details, among quaternary ammonium cations, we focused on poly(diallyldimethylammonium) chloride[24] (**P[DADMA][Cl]**), which was expected to exhibit

[a] *Institute of Multidisciplinary Research for Advanced Materials, Tohoku University, 2-1-1 Katahira, Aoba-ku, Sendai, Miyagi 980-8577, Japan. E-mail: oka@tohoku.ac.jp*
[b] *Department of Biomolecular Engineering, Graduate School of Engineering, Tohoku University, 6-6 Aoba, Aramaki, Aoba-ku, Sendai, Miyagi 980-8579, Japan*
[c] *NITTO BOSEKI CO., LTD., 2-4-1 Kojimachi, Chiyoda-ku, Tokyo 102-8489, Japan*
[d] *Carbon Recycling Energy Research Center, Ibaraki University, 4-12-1 Nakanarusawa, Hitachi, Ibaraki 316-8511, Japan*
[e] *Deuterium Science Research Unit, Center for the Promotion of Interdisciplinary Education and Research, Kyoto University, Yoshida, Sakyo-ku, Kyoto 606-8501, Japan*

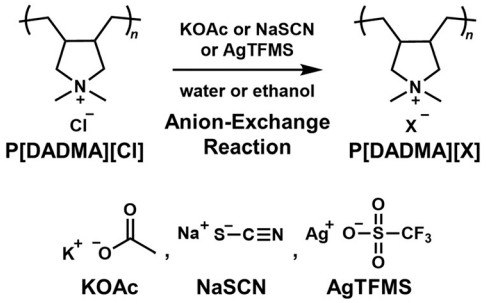

Fig. 1 Synthesis of PILs based on P[DADMA][Cl].

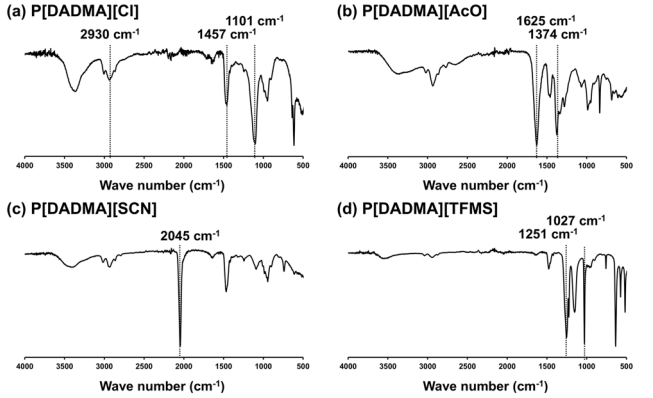

Fig. 2 FT-IR spectra of (a) P[DADMA][Cl], (b) P[DADMA][AcO], (c) P[DADMA][SCN], and (d) P[DADMA][TFMS].

particularly high CO_2 adsorption capacity owing to its exceptionally high ammonium cation density. To quantitatively elucidate the effect of counter anion size on CO_2 adsorption capacity, we also focused on three different-sized anions (AcO^-: 0.252 nm < SCN^-: 0.289 nm < trifluoromethane sulfonate ($TFMS)^-$: 0.304 nm) that are larger than Cl^- (0.214 nm) and performed anion-exchange reactions. Consequently, the purification of the obtained PILs *via* dialysis allowed for the first time the preparation of high-purity PILs (**P[DADMA][AcO]**, **P[DADMA][TFMS]**, **P[DADMA][SCN]**) that are free from residual impurities (Fig. 1). The CO_2 adsorption capacity of the obtained PILs increased in proportion to the size of the anion. This work provides new design principles for PILs towards efficient CO_2 absorbents.

Experimental section

Synthesis of P[DADMA][AcO]

P[DADMA][Cl] (1000 mg, 6.19 mmol) was added to ethanol (10 mL) and potassium acetate (607 mg, 6.19 mmol) was added at room temperature and stirred overnight. The reaction mixture was filtered and concentrated under reduced pressure using an evaporator. The resulting residue was dissolved in 10 mL of water, dialyzed in 1 L water for 24 h, and dried in a freeze dryer. After one day of drying, a yellow solid (117 mg, 0.63 mmol, 10%) was obtained. The synthesis methods for other PILs (**P[DADMA][SCN]** and **P[DADMA][TFMS]**) are described in the SI.

Results and discussion

1. PILs preparation

Each PIL (**P[DADMA][AcO]**, **P[DADMA][TFMS]**, **P[DADMA][SCN]**) was prepared by an anion-exchange reaction in solution using **P[DADMA][Cl]** as the starting material, following the procedure given in the experimental section and SI. Inorganic salts of several anions (KOAc, NaSCN, and AgTFMS) were selected for anion-exchange because of their high solubility in the reaction solvent and efficient reaction progress. In the anion-exchange reactions, the amount of inorganic salt was determined based on the solubility of the resulting byproduct in the reaction solvent. Specifically, an equimolar amount of inorganic salt was sufficient to drive the reaction to completion when the byproduct was insoluble in the reaction solvent, as its precipitation effectively shifted the equilibrium. Conversely, an excess amount was used when the byproduct was soluble. After the reaction, the removal of impurities *via* dialysis allowed us to yield high-purity PILs.

2. Characterization

As shown in Fig. 2 and 3, the progress of the anion-exchange was confirmed by the FT-IR and energy-dispersive X-ray spectroscopy (EDX) spectra. First, as shown in Fig. 2a as a representative example, the FT-IR spectra of all PILs exhibited peaks derived from the C–H stretching vibration (1457 cm^{-1}), C–H bending vibration (2930 cm^{-1}), and C–N stretching vibration (1101 cm^{-1}) of the polymer moiety[21] (Table S1). Subsequently, as shown in Fig. 2b, the FT-IR spectrum of **P[DADMA][AcO]** exhibited peaks derived from the COO^- antisymmetric stretching vibration (1625 cm^{-1}) and COO^- symmetric stretching vibration (1374 cm^{-1}) of AcO^-[21] (Table S2). As shown in Fig. 2c, the FT-IR spectrum

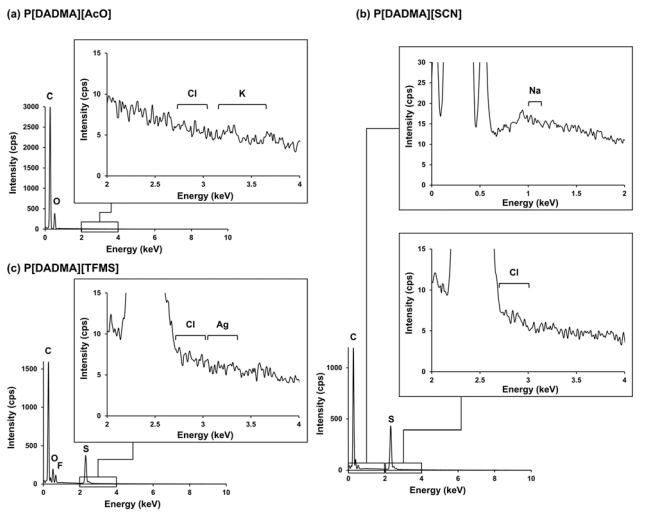

Fig. 3 EDX spectra of (a) P[DADMA][AcO], (b) P[DADMA][SCN], and (c) P[DADMA][TFMS].

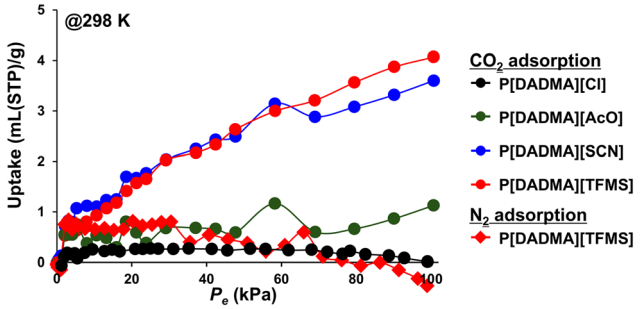

Fig. 4 CO_2 and N_2 adsorption isotherms of **P[DADMA][Cl]** (black), **P[DADMA][AcO]** (green), **P[DADMA][SCN]** (blue), and **P[DADMA][TFMS]** (red), measured at 298 K.

of **P[DADMA][SCN]** exhibited a peak corresponding to the CN stretching vibration (2045 cm^{-1}) of SCN^- [21] (Table S3). As shown in Fig. 2d, the FT-IR spectrum of **P[DADMA][TFMS]** exhibited peaks derived from the C–F stretching vibration (1251 cm^{-1}) and O═S═O stretching vibration (1027 cm^{-1}) of $TFMS^-$ [25] (Table S4).

As shown in Fig. 3, the EDX spectra of each **PIL** demonstrate the complete disappearance of Cl atoms derived from the starting material, **P[DADMA][Cl]**. These peak changes indicated the completion of the anion-exchange reaction. In addition, the same SEM-EDX spectra exhibited only peaks corresponding to the respective **PIL**s as products, indicating that impurities in the PILs were below the detection limit of SEM-EDX (0.1 wt%[26]). This result demonstrates that purification *via* dialysis after the anion-exchange reaction is effective for the synthesis of high-purity **PIL**s without impurities. To the best of our knowledge, this is the first time that such high-purity **PIL**s have been synthesized in **DADMA**-based **PIL**s. As shown in Fig. S1 and Table S5, the differential scanning calorimetry (DSC) curves of the PILs revealed glass transition temperatures (T_g) that varied depending on the counter anion. The T_g of **P[DADMA][Cl]** is consistent with previously reported values,[20] whereas the other **PIL**s exhibit lower T_g values. This trend is generally attributed to the increased size of the counter anions, which enhances free volume (space between polymer chains[27]) and facilitates segment motion.[28] As mentioned later, this increase in free volume also leads to increased CO_2 adsorption. Notably, **P[DADMA][AcO]** exhibited the lowest T_g despite its relatively small anion size. This is attributed to the strong interaction between AcO^- and electron-deficient sites[29] such as the methyl group of the **DADMA** backbone owing to the high hydrogen-bonding capability of AcO^-,[30] which inhibited the close packing between polymer chains.

3. Gas sorption properties

As shown in Fig. 4, the CO_2 adsorption capacity of each **PIL** was evaluated using the CO_2 adsorption isotherm at 298 K. As shown in Table 1, the CO_2 adsorption amounts followed the order: **P[DADMA][TFMS]** > **P[DADMA][SCN]** > **P[DADMA][AcO]** > **P[DADMA][Cl]**. This order corresponds to the size of the anions ($TFMS^-$ > SCN^- > AcO^- > Cl^-). As shown in Fig. S2, the CO_2 adsorption capacity was found to increase in general proportion to the anion size. This result supports that larger counter anions increase the CO_2 adsorption capacity by contributing to the expansion of the free volume and promoting CO_2 diffusion within the **PIL**s.[31] In a previous work, **PIL**s (**P[DADMA][AcO]**) bearing the more basic AcO^- as the counter anion exhibited higher adsorption capacity than that of $TFMS^-$, indicating some contribution of chemical affinity based on the counter anion's basicity.[21] However, this result likely includes the influence of residual inorganic salts that can fill the free volume. In contrast, the high-purity **PIL**s obtained in this work revealed the opposite trend, with **P[DADMA][TFMS]** exhibiting a higher CO_2 adsorption than that of **P[DADMA][AcO]**. This result supports the conclusion that CO_2 adsorption on high-purity **PIL**s is governed by the free volume derived from the size of the counter anion, which becomes more dominant than the chemical affinity derived from the basicity of the counter anion. As shown in Fig. S3, the CO_2 adsorption capacities of **P[DADMA][TFMS]** before (**P[DADMA][TFMS]** with 0.12 atomic% of Ag atoms) and after purification by dialysis were compared. The CO_2 adsorption capacity of the unpurified **P[DADMA][TFMS]** (3.56 mL g^{-1} at 100 kPa) was lower than that of the purified, high-purity **P[DADMA][TFMS]** (4.04 mL g^{-1} at 100 kPa), supporting the inhibition of CO_2 adsorption caused by impurities remaining in the **PIL**s. In addition, as shown in Fig. 4 and S4, the N_2 adsorption isotherms at 298 K indicated negligible N_2 adsorption for all **PIL**s, demonstrating that the type of anion in the **PIL**s did not significantly affect the N_2 adsorption capacity. Therefore, this work confirms that improving the CO_2 adsorption capacity by the designing of anions in **PIL**s also contributes to enhancing the adsorption selectivity of CO_2/N_2.

Table 1 CO_2 and N_2 adsorption amount of PILs

Sample	Anion radius[a]/nm	V_{CO_2}[b]/mL g^{-1}	V_{N_2}[c]/mL g^{-1}
P[DADMA][Cl]	0.214	0.155	—
P[DADMA][AcO]	0.252	1.13	0.449
P[DADMA][SCN]	0.289	3.60	0.502
P[DADMA][TFMS]	0.304	4.07	—

[a] Estimated based on density functional theory (**DFT**) calculations (B3LYP/6-31+G(d,p)). [b] CO_2 adsorption amount at 100 kPa. [c] N_2 adsorption amount at 100 kPa.

Conclusions

In this work, we successfully synthesized three high-purity **PIL**s (**P[DADMA][AcO]**, **P[DADMA][TFMS]**, **P[DADMA][SCN]**) from **P[DADMA][Cl]** as the starting material by anion-exchange and dialysis. These **PIL**s exhibited enhanced CO_2 adsorption capacity proportional to the size of their counter anions, and **P[DADMA][TFMS]** exhibited seven-times higher adsorption capacity than that of the starting material **P[DADMA][Cl]**. This is attributed to the large anions expanding the free volume of the **PIL**s, facilitating CO_2 diffusion. This work truly demonstrates

that CO_2 adsorption capacity can be enhanced by designing the counter anions in **PIL**s.

Conflicts of interest

There are no conflicts to declare.

Data availability

The supporting data has been provided as part of the supplementary information (SI).

Supplementary information: Fig. S1–S4 and Tables S1–S5, and further experimental details. See DOI: https://doi.org/10.1039/d5re00535c.

Acknowledgements

This work was partially supported by Grants-in-Aid for Scientific Research (no. JP23K17945, JP23H03827, JP24K01552, and JPJSBP120258801) from MEXT, Japan. This work was partially supported by the Environment Research and Technology Development Fund (JPMEERF20241RA4) of the Environmental Restoration and Conservation Agency provided by the Ministry of the Environment of Japan. KO also acknowledges support from the Shorai Foundation for Science and Technology, the TEPCO Memorial Foundation, the Amano Industry Technology Laboratory, Sugiyama Houkoukai, the Yamada Science Foundation, the Kenjiro Takayanagi Foundation, the Kansai Research Foundation for Technology Promotion, the Yashima Environment Technology Foundation, the JACI Prize for Encouraging Young Researcher, the Iketani Science and Technology Foundation, the Foundation for Interaction in Science & Technology, and the Kato Foundation for Promotion of Science (KS-3416).

References

1 K. Fukumoto, M. Yoshizawa and H. Ohno, *J. Am. Chem. Soc.*, 2005, **127**, 2398–2399.
2 M. Yoshizawa, W. Xu and C. A. Angell, *J. Am. Chem. Soc.*, 2003, **125**, 15411–15419.
3 K. Tanaka, F. Ishiguro and Y. Chujo, *J. Am. Chem. Soc.*, 2010, **132**, 17649–17651.
4 H. Sei, Y. N. Kanasaki, K. Oka, N. Tohnai, Y. Kohno and T. Makino, *ACS Omega*, 2023, **8**, 21154–21161.
5 R. Inaba, T. Imai, S. Kitajima, H. Kasai, K. Oka, R. Hifumi, I. Tomita, M. Yoshizawa-Fujita, K. Naka and H. Imoto, *Chem. Commun.*, 2024, **60**, 14022–14025.
6 M. Hirao, K. Ito and H. Ohno, *Electrochim. Acta*, 2000, **45**, 1291–1294.
7 M. Yoshizawa, W. Ogihara and H. Ohno, *Polym. Adv. Technol.*, 2002, **13**, 589–594.
8 S. Al-Sodies, A. M. Asiri, A. Khan, K. A. Alamry and M. A. Hussein, *Eur. Polym. J.*, 2024, **205**, 112719.
9 M. Zhu and Y. Yang, *Green Chem.*, 2024, **26**, 5022–5102.
10 N. V. Plechkova and K. R. Seddon, *Chem. Soc. Rev.*, 2008, **37**, 123–150.
11 T. Welton, *Biophys. Rev.*, 2018, **10**, 691–706.
12 M. Hasib-ur-Rahman, M. Siaj and F. Larachi, *Chem. Eng. Process.: Process Intesif.*, 2010, **49**, 313–322.
13 W. Qian, J. Texter and F. Yan, *Chem. Soc. Rev.*, 2017, **46**, 1124–1159.
14 Z. Dai, R. D. Noble, D. L. Gin, X. Zhang and L. Deng, *J. Membr. Sci.*, 2016, **497**, 1–20.
15 S. Chen, Y. Chao, J. Wu, H. Ye, X. Luo and Z. Liang, *Ind. Eng. Chem. Res.*, 2022, **61**, 11953–11963.
16 Y. Xie, Q. Sun, Y. Fu, L. Song, J. Liang, X. Xu, H. Wang, J. Li, S. Tu, X. Lu and J. Li, *J. Mater. Chem. A*, 2017, **5**, 25594–25600.
17 S. M. Morozova, A. S. Shaplov, E. I. Lozinskaya, D. Mecerreyes, H. Sardon, S. Zulfiqar, F. Suárez-García and Y. S. Vygodskii, *Macromolecules*, 2017, **50**, 2814–2824.
18 Y. Ye and Y. A. Elabd, *Polymer*, 2011, **52**, 1309–1317.
19 M. G. Cowan, D. L. Gin and R. D. Noble, *Acc. Chem. Res.*, 2016, **49**, 724–732.
20 J. Tang, H. Tang, W. Sun, M. Radosz and Y. Shen, *J. Polym. Sci., Part A: Polym. Chem.*, 2005, **43**, 5477–5489.
21 R. S. Bhavsar, S. C. Kumbharkar and U. K. Kharul, *J. Membr. Sci.*, 2012, **389**, 305–315.
22 X. Ma, L. Li, R. Chen, C. Wang, K. Zhou and H. Li, *Fuel*, 2019, **236**, 942–948.
23 T. Schuett, R. Geitner, S. Zechel and U. S. Schubert, *Macromolecules*, 2021, **54**, 9410–9417.
24 A. Silva, R. V. Barrulas, M. C. Corvo and M. Zanatta, *J. Environ. Chem. Eng.*, 2023, **11**, 110882.
25 J. Golding, S. Forsyth, D. R. MacFarlane, M. Forsyth and G. B. Deacon, *Green Chem.*, 2002, **4**, 223–229.
26 P. C. Guyett, D. Chew, V. Azevedo, L. C. Blennerhassett, C. Rosca and E. Tomlinson, *J. Anal. At. Spectrom.*, 2024, **39**, 2565–2579.
27 M. S. Shannon, J. M. Tedstone, S. P. O. Danielsen, M. S. Hindman, A. C. Irvin and J. E. Bara, *Ind. Eng. Chem. Res.*, 2012, **51**, 5565–5576.
28 H. Tang, J. Tang, S. Ding, M. Radosz and Y. Shen, *J. Polym. Sci., Part A: Polym. Chem.*, 2005, **43**, 1432–1443.
29 A. R. Biery and D. M. Knauss, *Mater. Today Chem.*, 2022, **26**, 101251.
30 Y. Xu, Y. Xu, C. Sun, L. Zou and J. He, *Eur. Polym. J.*, 2020, **133**, 109768.
31 J. Tang, Y. Shen, M. Radosz and W. Sun, *Ind. Eng. Chem. Res.*, 2009, **48**, 9113–9118.

